Available online at www.sciencedirect.com
ScienceDirect
Nuclear Instruments and Methods in Physics Research A 592 (2008) 434–450
NUCLEAR INSTRUMENTS & METHODS IN PHYSICS RESEARCH Section A
www.elsevier.com/locate/nima

Identification of isotope lines in two-dimensional spectra of nuclear multifragmentation

Miroslav Morháč*, Martin Veselský

Institute of Physics, Slovak Academy of Sciences, Dúbravská cesta 9, 845 11 Bratislava, Slovakia

Received 18 February 2008; received in revised form 18 March 2008; accepted 1 April 2008
Available online 10 April 2008

Abstract

In the paper, we propose new algorithm of the determination of ridges in two-dimensional spectra of nuclear multifragmentation. The algorithm is based on slicing the raw data and their subsequent linearization. To find corresponding points, which contribute to the estimate of fitted line parameters in sparsely distributed linearized data, as well as to span gaps and decrease statistical fluctuations, the algorithm is based on smoothing technique using second derivatives of Gaussian. In the paper, we analyze and study thoroughly the influence of various parameters. Illustrative examples prove in favor of the proposed algorithm.

PACS: 07.05.Kf; 29.85.+c

Keywords: Fragment energy loss spectra; Smoothed second derivatives; Deconvolution

1. Introduction

In the nuclear reactions well above Coulomb barrier, multiple charged particles are emitted in a wide angular range. In order to detect all charged particles emitted during the reaction, multi-detector arrays consisting of many charged particle telescopes emerged, with optimized choice of angular coverage (ideally $4-\pi$), granularity and detection thresholds. An important step in the off-line analysis of data from the multi-detector arrays with large angular coverage is to identify as many fragment species as possible. The method of isotope identification is based on well-known particle telescope technique in which the isotopes are resolved in two-dimensional (2D) $\Delta E-E$ spectra of energy losses in two detectors (typically a thin one followed by a thick one). The method needs to be applied to all detectors, which makes the analysis a highly repetitive task and methods allowing automation are preferable.

Main task of the analysis is to parametrize the relation of energy losses to observed electronic signals in two detectors. Charge identification was achieved in the work [1] by obtaining analytical fit of calculated energy losses for specific fragment species and by mapping of resulting matrix on a set of sampled experimental lines using the minimization procedure, with particle charge being the minimization parameter. In other works [2,3] the subset of lines with a priori known mass and charge was sampled and the parameters relating the energy loss to electronic signals are obtained by minimization procedure. Such method enables to carry out identification and energy calibrations simultaneously using a minimization procedure applied to 2D spectra. For instance, in the work [2] the lines for three known isotopes (typically the most characteristic isotopes such as ^{1}H, ^{4}He, ^{9}Be) are assigned in the experimental spectra and calibration is carried out by a minimization procedure where these lines are fitted to corresponding calculated energy losses for a given $\Delta E-E$ telescope. The calibrations coefficients are thus obtained as optimum values of minimization parameters and identification can be achieved after superimposing the calculated energy loss lines onto experimental spectra. In this

*Corresponding author. Tel.: +421 2 59410536; fax: +421 2 54776085.
E-mail address: Miroslav.Morhac@savba.sk (M. Morháč).

0168-9002/$ - see front matter © 2008 Elsevier B.V. All rights reserved.
doi:10.1016/j.nima.2008.04.002

procedure, the initial assignment of the selected isotope lines required human intervention, since the lines had to be drawn by hand. To make such procedure fully automatic, one needs an algorithm which would recognize and tabulate some of the isotope lines in the 2D spectra (manifested as non-linear ridges). In the works [4,5], algorithms were proposed to recognize individual spectral lines in the 2D spectra, using the smoothing and differentiation methods [4] or neural network approach [5]. Separation of experimental lines with different atomic number was achieved. An alternative algorithm for recognition of isotope lines is proposed in the present work.

2. Proposal and formulation of the algorithm

During the process of nuclear multifragmentation, multiple charged particles are produced. An important step in the analysis of data of this kind is to identify correctly the fragment species. As opposed to the identification of self-standing peaks (one-, or multidimensional, e.g. in γ-ray spectra) here we have to find also the

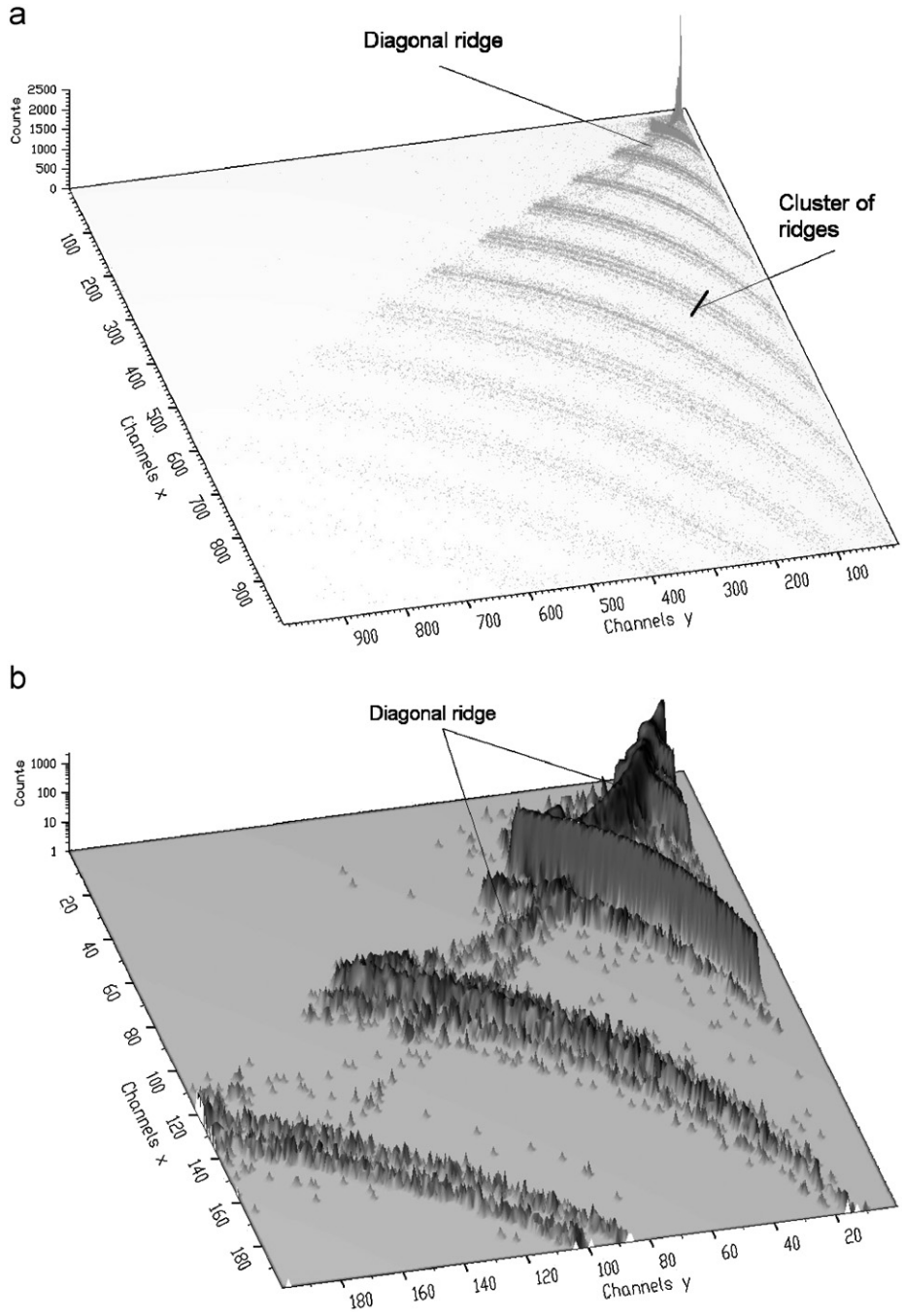

Fig. 1. (a) An example of two-dimensional spectrum of nuclear multifragmentation, and its detail. (b) The variables x and y represent electronic signals originating from a pair of silicon detectors and recorded by the corresponding ADCs.

correspondence among the identified local maxima belonging to the same ridge.

Let us now analyze the problems connected with the process of determination of ridges in the spectra of nuclear multifragmentation. To make things clear we shall accompany our considerations with an illustrative example. In Fig. 1a one can see 2D energy loss spectrum from the telescope, consisting of two silicon detectors, of the size 1000×1000 channels. The data originate from a pair of silicon detectors with respective thickness 150 and 500 μm and the electronic gains were adjusted to equalize amplitudes in both electronic channels. The variables x and y represent electronic signals recorded by the corresponding ADCs. The shape of the spectral lines in the spectrum is a usual one for such type of detectors. The empty region on the top left is caused by the punch through of the second silicon detector, which defines a maximum energy. Particles with higher energies are not shown in the plot, except few events where anticoincidence signal was not detected (represented by weak line where energy losses in both silicon detectors decrease simultaneously). The isotopic resolution in the spectrum is achieved up to the $Z = 10$.

To illustrate the complexity and statistical fluctuations in the data in Fig. 1b we show detail at the beginning of the coordinate system. We have to determine ridges of corresponding points from very sparsely distributed 2D experimental data. Besides, the spectra of nuclear multifragmentation are extremely noisy.

At the first glance at the data in Fig. 1a one can observe that the data vary over many orders of magnitude going from thousands of counts at the beginning of the spectrum to tens or ones in its rest. To compress the dynamic range in channel counts and to suppress the effect of the noise in the data sets a series of mathematical operators were studied in Ref. [6]. Taking the square root, then using the natural log operator twice (LLS) was claimed to yield the best results. LLS operator is applied to every channel $y(i)$

$$v(i) = \log[\log(\sqrt{y(i)+1}+1)+1] \quad (1)$$

The application of LLS operator is an important starting point in the identification of ridges in the spectra of nuclear multifragmentation. In Fig. 2 we present the spectrum from Fig. 1 after application of LLS operator.

The procedure of the identification of non-linear ridges can be split down into several points. The first step of the non-linear ridges identification is their quasi-linearization. Though it is possible to do it in various ways (e.g. to transform data to polar coordinates) we proposed rather simple approach based on the slicing of original data from a given point according to Fig. 3. Let us start slicing at the point A and go along the diagonal to the beginning of the original coordinate system. The distance from the point A represents the parameter S. In this way we get the slice number 0. When changing successively the end points of the slices to 1, 2,…, $N-1$ on both axes x_1 and x_2 we get slices R and L, respectively. The new S coordinate is the distance from the point A, while the new R and L coordinates represent the number of the slice or in other words the length of the segment intercepted by the slice on the axis x_1 and x_2, respectively.

Due to the outlined coordinate transformation we obtain data in two halfplanes arranged predominantly in quasi-linear directions. The curvatures on the left and right sides of the lines are different. Therefore, the angles of the arrangements in both halfplanes are also different. Spectrum from Fig. 2 sliced according to the algorithm of slicing outlined in Fig. 3 is shown in Fig. 4. One can

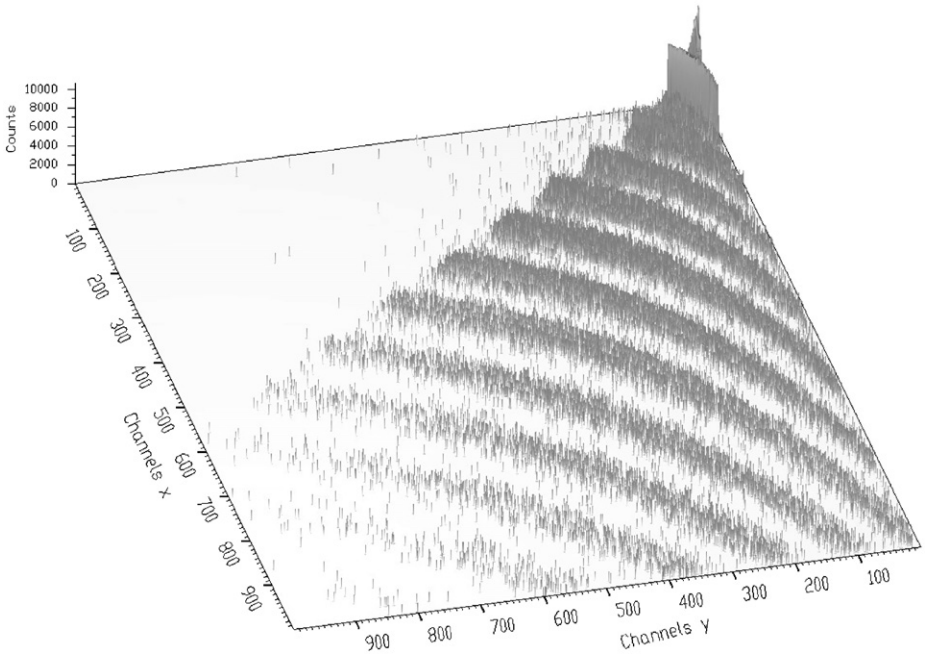

Fig. 2. Spectrum from Fig. 1 after application of LLS operator.

observe that the trends in both halfplanes can be well approximated by straight lines one for each halfplane.

On the other hand the linearized data in Fig. 4 are also distributed sparsely. From the above mentioned considerations one can conclude that the algorithm of ridges identification should

(a) suppress statistical fluctuations,
(b) glue together points in the linear directions,
(c) separate linearized ridges from each other (in vertical direction),
(d) ignore other artificial objects (e.g. diagonal ridge—see Fig. 1).

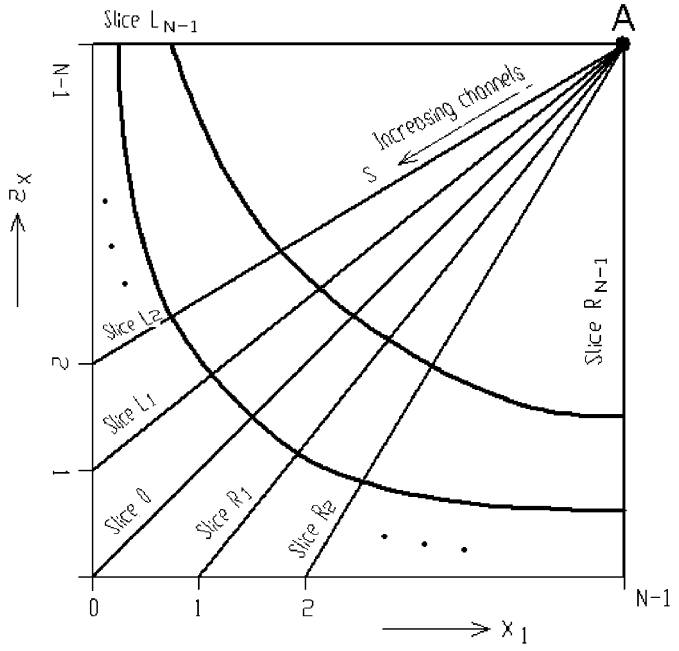

Fig. 3. Principle of slicing of two-dimensional spectrum.

To suppress statistical fluctuations in the linearized data we employed second derivative filtration technique. Using this technique together with suppression of noise we can carry out peak searching in one-dimensional (1D) slices. There exist a lot of algorithms of this, at the first glance very simple, but in its essence very complicated and complex problem [7–10]. In Refs. [11,12] so-called correlation technique emerged. It is based on the second derivative of the Gaussian as the convolution function, called also the correlator

$$c(j) = \frac{j^2 - \sigma^2}{\sigma^4} \exp\left(-\frac{j^2}{2\sigma^2}\right) = \frac{\mathrm{d}^2}{\mathrm{d}x^2} \exp\left(-\frac{x^2}{2\sigma^2}\right)_{x=j} \tag{2}$$

where σ determines the width of searched peaks. The convolution of input data x with correlator c yields

$$y(i) = \sum_{k=0}^{i} x(k)c(i-k), \quad i = 0, 1, \ldots, N-1. \tag{3}$$

The local minimums of $y(j)$ identify positions of peaks. As we need to carry out the peak smoothing and searching in several directions and moreover we also need to confine the peak regions of potential peak candidates to finite intervals we propose a technique based on inverted positive second derivative (IPSD) of the Gaussian

$$p(j) = \begin{cases} -y(j) & \text{if } y(j) < 0, \\ 0 & \text{otherwise.} \end{cases} \tag{4}$$

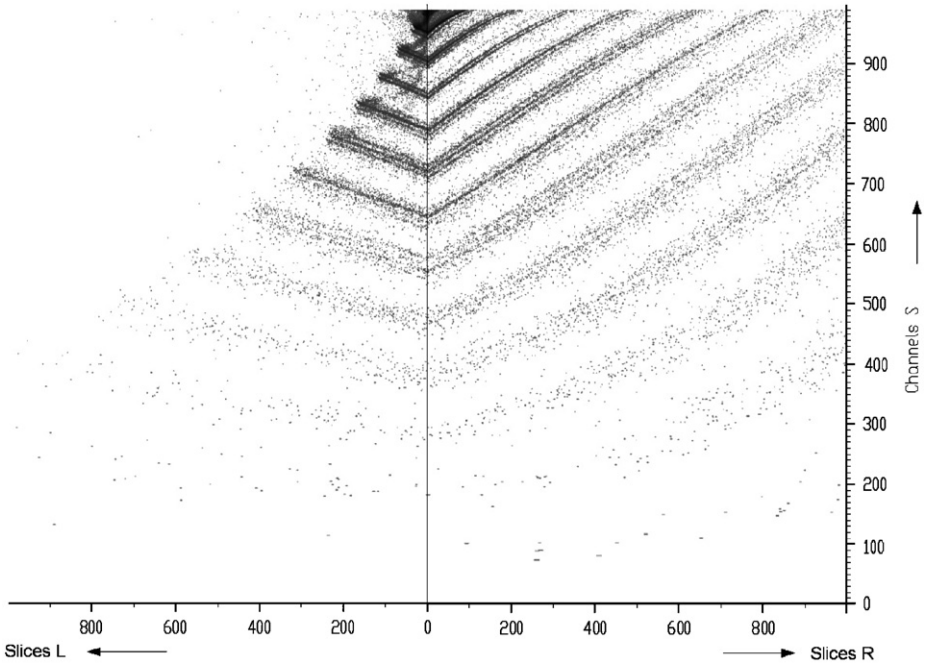

Fig. 4. Spectrum from Fig. 2 sliced and linearized according to the algorithm outlined in Fig. 3.

The example of the second derivative and IPSD of the Gaussian for $\sigma = 20$ is presented in Fig. 5a and b, respectively.

Now let us apply the IPSD algorithm of filtering ($\sigma = 20$) to the columns of linearized data shown in Fig. 4. We get data smoothed in vertical directions given in Fig. 6.

To glue the slices together we repeat the same procedure in horizontal direction with $\sigma_2 = 30$. We obtain data presented in Fig. 7.

Now we need to determine directions of ridges in both halfplanes. To determine seed points of the direction lines we can find maximums in the slice 0 (Fig. 8).

We find sequences of maximums in neighboring slices in both directions. By fitting the sequences with lines and taking the estimates with the smallest chi-squares we get direction angles of dominant ridges in both directions (Fig. 9).

In the directions determined by these angles we carry out the smoothing of original (non-smoothed) sliced data employing convolution technique with Gaussian filter with given σ_3. To span gaps in sparsely distributed data and to determine intrinsically the correspondence among experimental points in the spectrum the parameter σ_3 should be set to an appropriate value. Analogously to Eq. (3) the

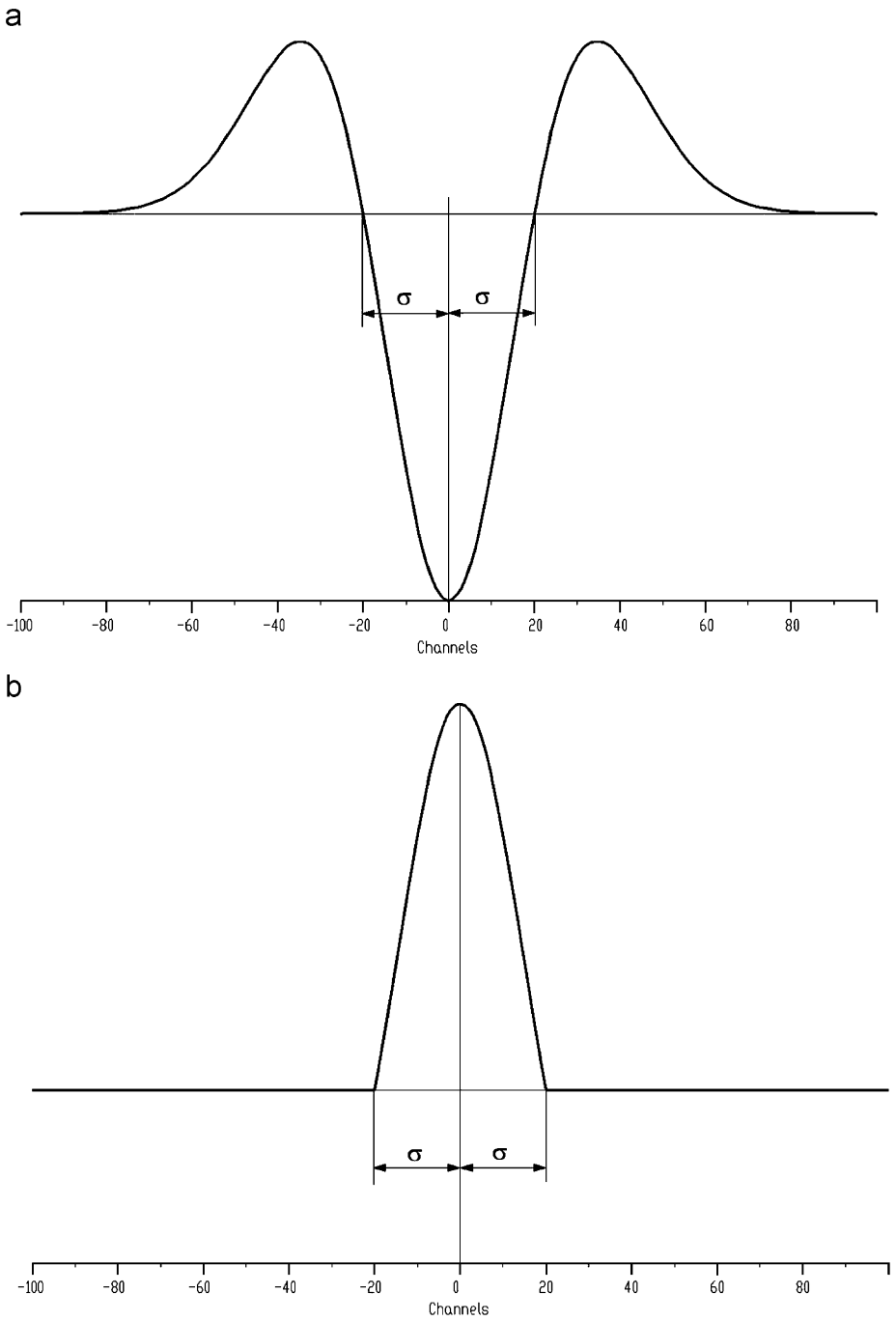

Fig. 5. The example of the second derivative (a) and inverted positive second derivative (b) of the Gaussian for $\sigma = 20$.

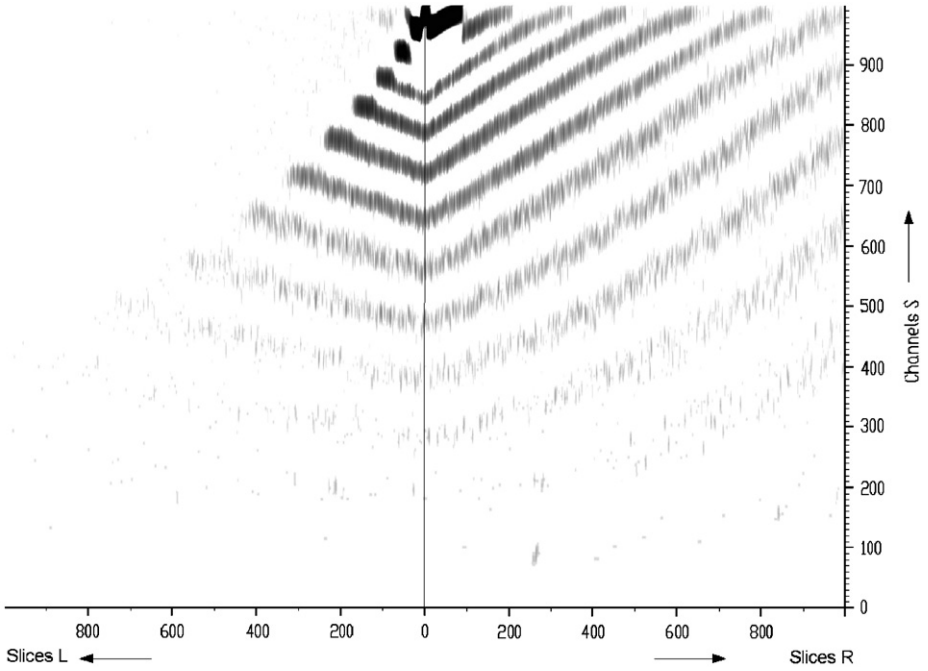

Fig. 6. Data from Fig. 4 smoothed vertically with IPSD filter with $\sigma_1 = 20$.

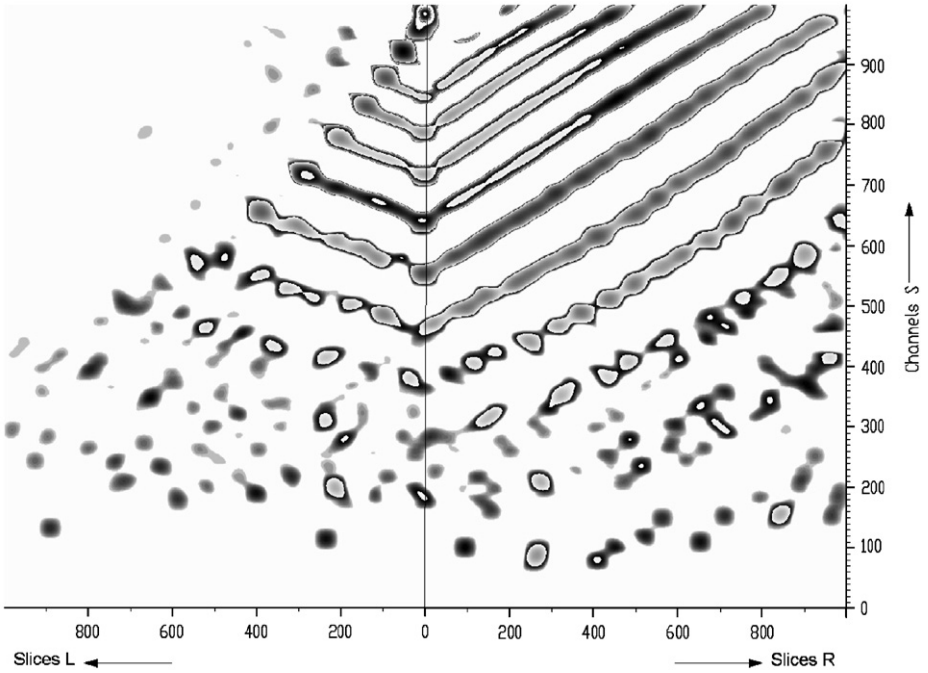

Fig. 7. Data from Fig. 6 smoothed in horizontal direction ($\sigma_2 = 30$).

convolution of input data x with filter g is

$$y(i) = \sum_{k=0}^{i} x(k)g(i-k), \quad i = 0, 1, \ldots, N-1. \tag{5}$$

Further, let us return back to our example data in Fig. 4. Let us find the directions in both halfplanes and smooth the data in these directions using Eq. (5). The result of this operation for $\sigma_3 = 30$ is given in Fig. 10.

The points in corresponding ridges are connected. However, we need to separate peaks and smooth data in the vertical direction. Moreover, we need to confine data to regions of peaks and to eliminate data outside these regions. Therefore, we employ again the IPSD algorithm

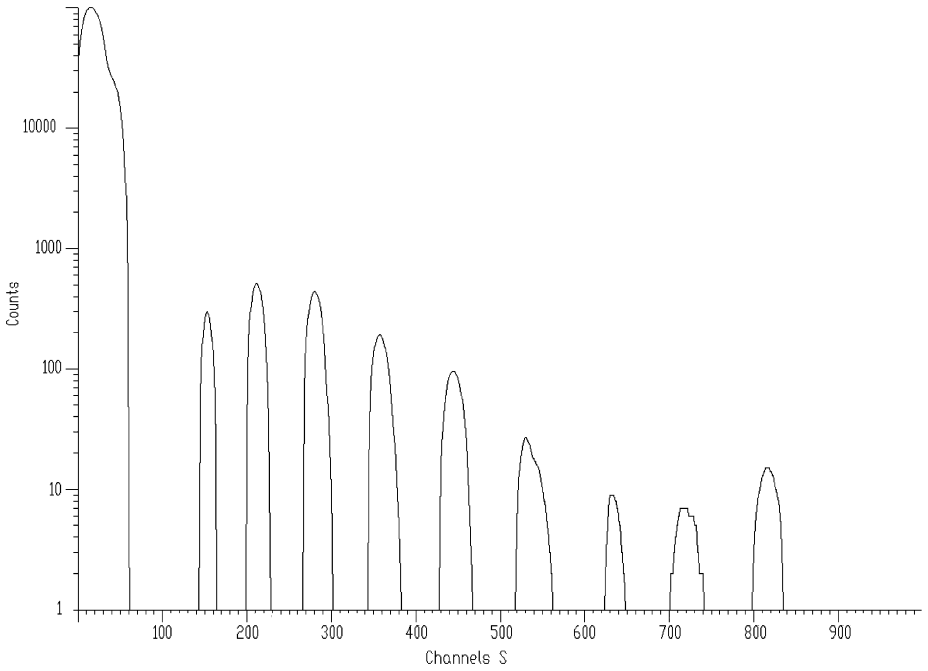

Fig. 8. Slice 0 from the data from Fig. 7.

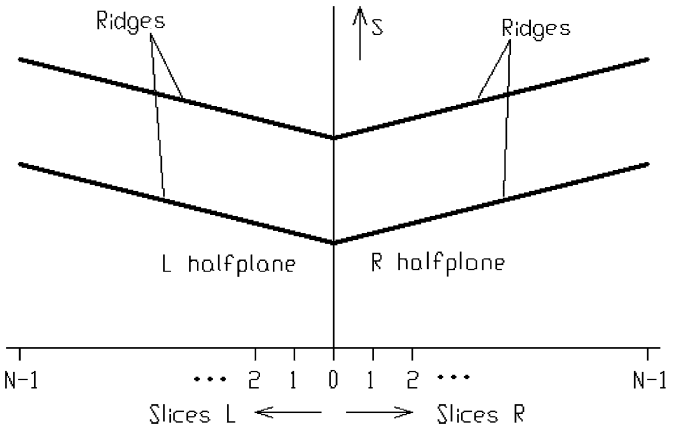

Fig. 9. Linearized ridges in sliced and twice smoothed two-dimensional spectrum.

given by Eqs. (2)–(4) with $\sigma_4 = 20$. We get smoothed data in both directions with connected points in corresponding ridges (Fig. 11).

Analogously to Fig. 8 we can take slice 0. The local maximums in this data can serve as seed points to find corresponding points in ridges in both halfplanes. We look for the local maximums (in vertical direction) in the neighboring slices. The principle and scanning window for the right halfplane and for the first ridge is given in Fig. 12. We assume that starting from the point A we have already found the points belonging to the ridge until point B. Now we have to find the next point within the outlined skew window. The height of the window is $2 \cdot \sigma_4$, its width is σ_3 and its slope is given by the direction angle for the right halfplane. If we find a maximum in this window we take it to be the ridge point and move the scanning window to right and repeat the scanning for the next point. Otherwise, we take the point B to be the last point of the ridge and we proceed to the next ridge. In this way we can determine all ridges.

Finally, in the last step we transform the ridges back to the original space of the 2D spectrum. The result of our example data is given in Fig. 13.

Let us summarize and express the above described algorithm of the identification of non-linear ridges concisely in several points:

(a) To compress the dynamic range of the channel counts apply the LLS operator to the spectrum data according to Eq. (1).
(b) The next step of the non-linear ridges identification is their quasi-linearization. We propose rather simple approach based on the slicing of original data from a given point according to Fig. 3.
(c) We obtain data in two halfplanes arranged predominantly in quasi-linear directions. However, the angles of the arrangements in both halfplanes are different. To suppress statistical fluctuations in the data we employed IPSD technique defined in Eqs. (2)–(4). We carry out smoothing using IPSD of Gaussian with given σ_1 separately for every slice (vertically in Fig. 3) in both halfplanes.
(d) To span gaps and decrease statistical fluctuations in the data in the horizontal direction we employ again IPSD technique (parameter σ_2).
(e) We find local maximums in the slice 0 greater than a threshold value (given in percentage of the maximum value in the slice 0) and use them as seed points for the

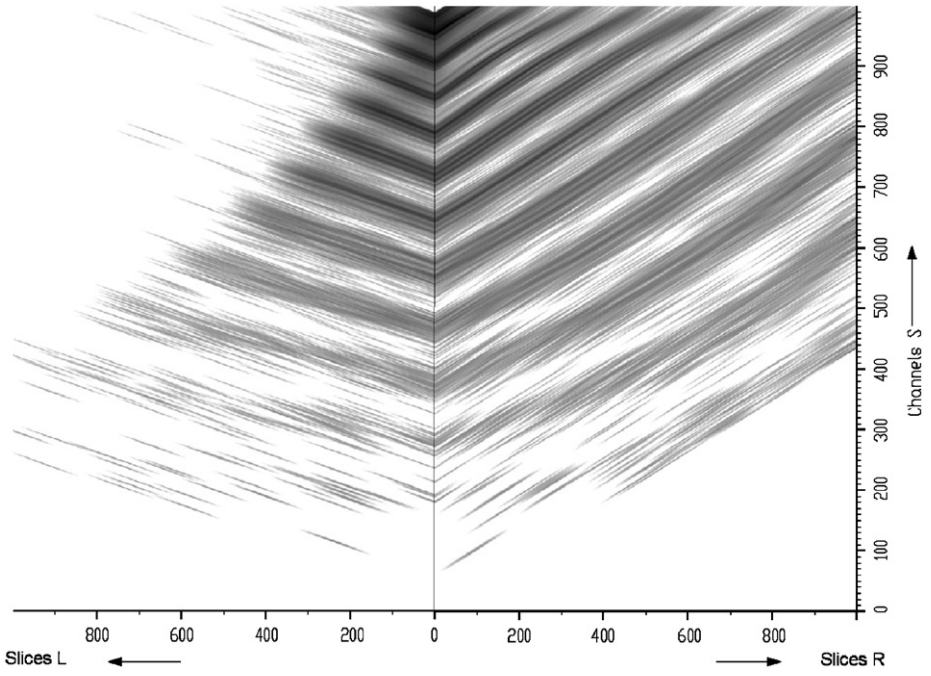

Fig. 10. Data from Fig. 4 after Gaussian smoothing in the direction of ridges $\sigma_3 = 30$.

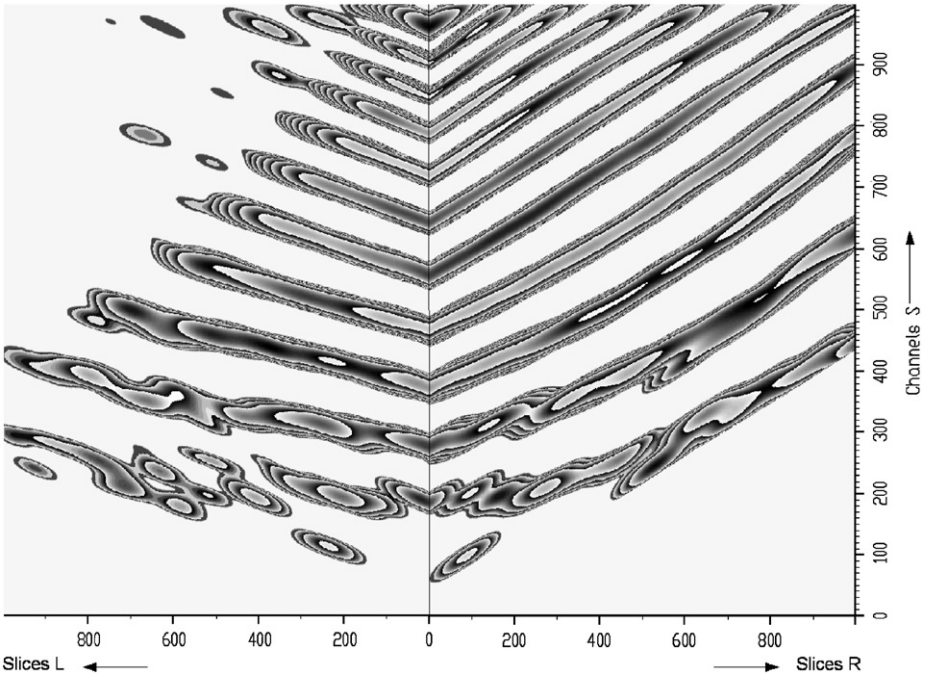

Fig. 11. Data from Fig. 10 after application of IPSD filter with $\sigma_4 = 20$.

determination of dominant directions in both halfplanes.

(f) In the next step, we find dominant directions of lines in both halfplanes by fitting corresponding local maxima in the smoothed inverted positive SSD data. We obtain direction angles for both halfplanes (see Fig. 9).

(g) In the directions determined by these angles we carry out the smoothing of original (non-smoothed) sliced data employing convolution technique (5) with Gaussian filter with a given σ_3. The parameter σ_3 influences smoothness of the estimated ridges.

(h) Further, the data smoothed in the dominant directions are submitted to another smoothing in the vertical direction S with IPSD of Gaussian with σ_4.

(i) To identify seeds of ridges in the column number 0 we find local maxima.

(j) In the last but one step we have to determine neighboring points (maximums) belonging to one ridge. We look for neighboring maximums in both direction angles. Let us assume we have found maximum in the right halfplane in the point (x_1, y_1) we look for the maximum in the column $(x = x_1+1,\ y \in \langle y_1-\sigma_4,\ y_1+\sigma_4\rangle)$. Nevertheless, even among maximums of twice smoothed data, there can be gaps. To span these possible gaps we search for the maximums within the quadrangle $(x = x_1+i,\ y \in \langle y_1-\sigma_4+k_r\cdot i,\ y_1+\sigma_4+k_r\cdot i\rangle)$, $i \in \langle 1,\ \sigma_3\rangle$. The width of the quadrangle is given by appropriate coefficients σ for smoothing in the direction of ridges and the last vertical smoothing. The situation for the left halfplane is analogous. The principle of looking for next corresponding local maximum is illustrated in Fig. 12.

(k) Finally we transform back the ridges points to original 2D spectrum.

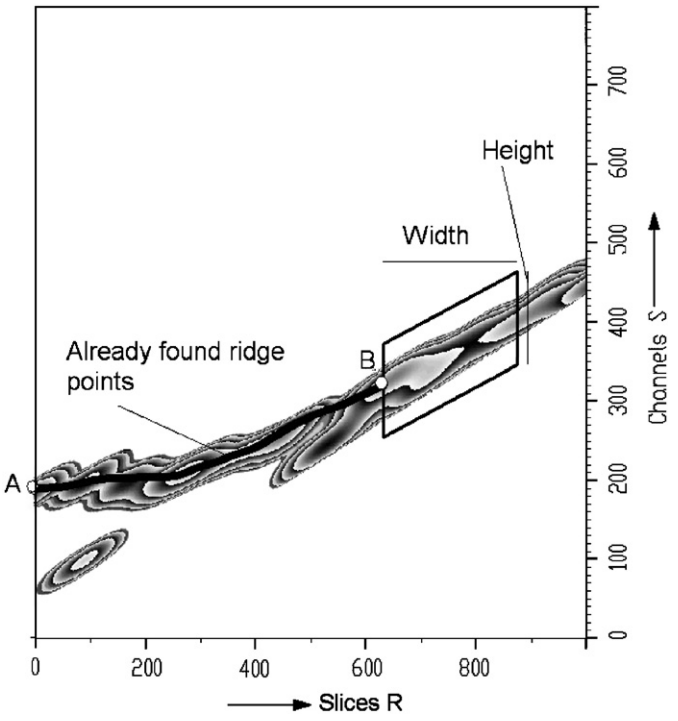

Fig. 12. Principle of searching for neighboring maximums in vertical slices.

3. Discussion and results

Crucial point of the above described algorithm is linearization of data in the transformed domain. To compare the proposed method with the transformation to polar coordinates, which is an alternative to the suggested algorithm outlined in Fig. 3, we introduce the example with the same data from Fig. 2. In Fig. 14a we present data from Fig. 2 transformed to polar coordinates. Here the transition from the right halfplane to the left one is much smoother than in the previous method. On the other hand the data cannot be linearized so smoothly, i.e., one can observe a greater non-linearity in appropriate ridges.

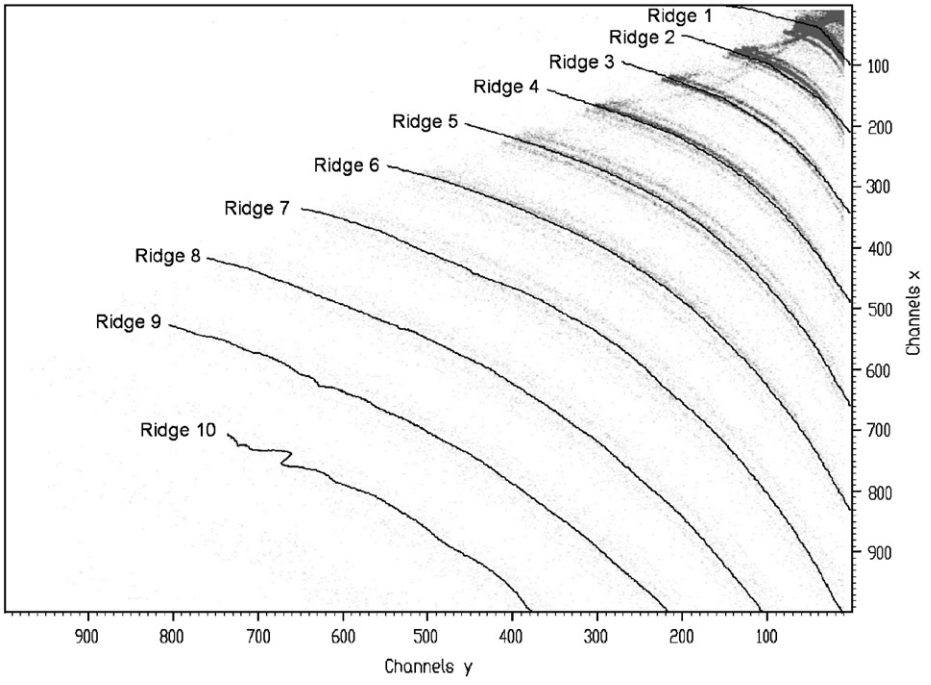

Fig. 13. Two-dimensional spectrum of nuclear multifragmentation with determined ridges (parameters $\sigma_1 = 20$, $\sigma_2 = 30$, $\sigma_3 = 30$, $\sigma_4 = 20$).

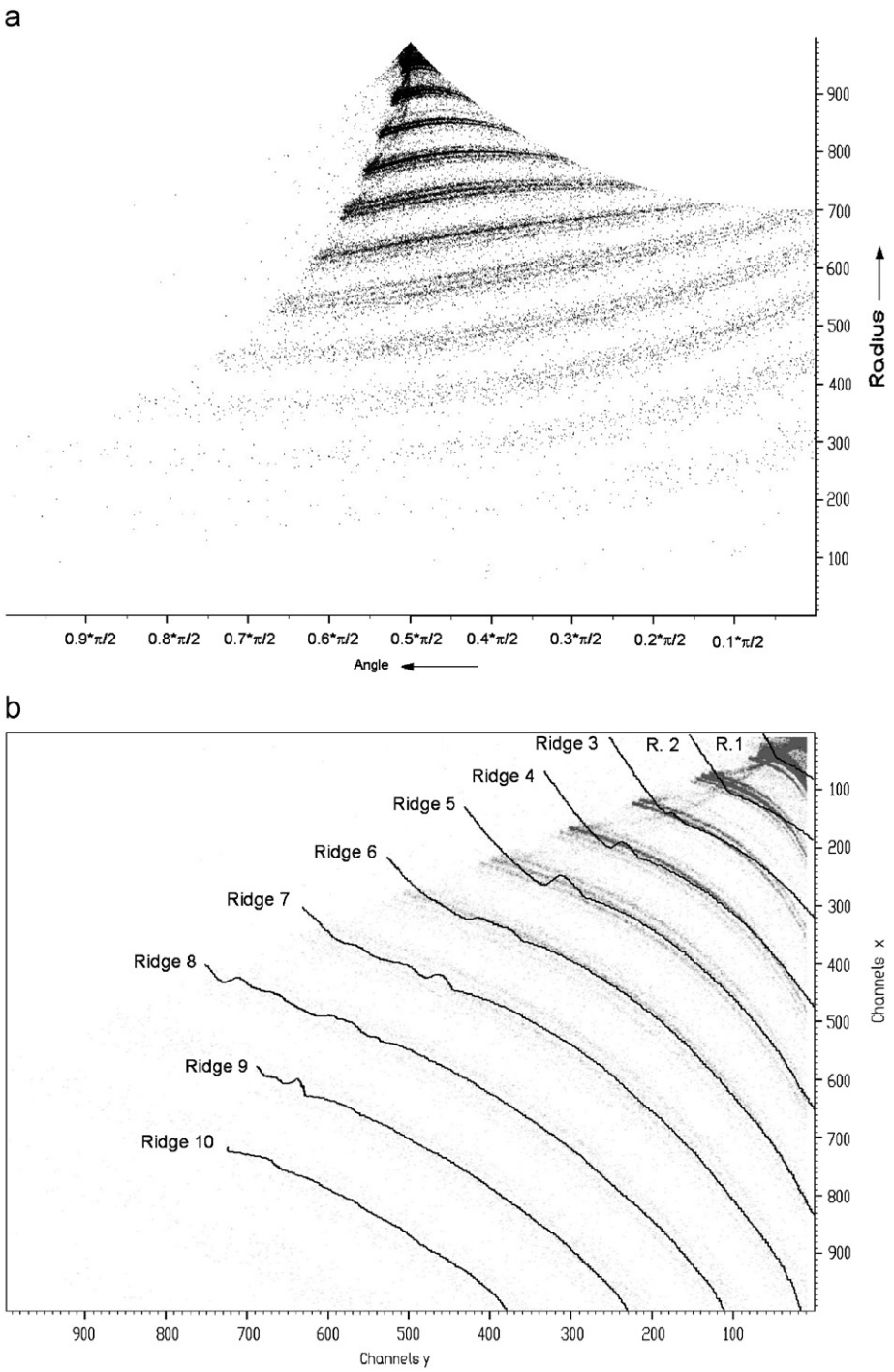

Fig. 14. (a) Transformation of spectrum from Fig. 2 to polar coordinates (b) and identified ridges transformed back to the original spectrum.

This results in non-acceptable estimate of the ridges given in Fig. 14b.

Now let us study the influence of the parameters (σ_1, σ_2, σ_3, σ_4 and threshold) to the estimation of the ridges. Though by tuning these parameters some improvements for polar model of linearization can be achieved in the following examples we shall consider only slicing model of linearization. The first two parameters σ_1, σ_2 are used for the filtration of linearized data in vertical and horizontal direction, respectively, by employing IPSD algorithm. Filtered data are subsequently used for the determination of dominant directions in these data. The algorithm is rather independent and robust to the changes of these parameters. We have studied the influence of σ_1, σ_2

by changing them in the range $\langle 5, 50 \rangle$. The estimates practically coincide with the result shown in Fig. 13.

Further let us analyze the influence of the parameter σ_3. Through the use of this parameter one can control smoothness of the estimated ridges. The examples for $\sigma_3 = 5, 10, 20, 50$ are illustrated in Fig. 15. With increasing σ_3 the estimated curves are getting smoother but on the other hand, one can observe undesirable slight distortion of their shapes on the right-hand side for the ridges 2, 3 and 4.

When comparing the results achieved in Figs. 13, 14b and 15 we see that the algorithm is able to discover main

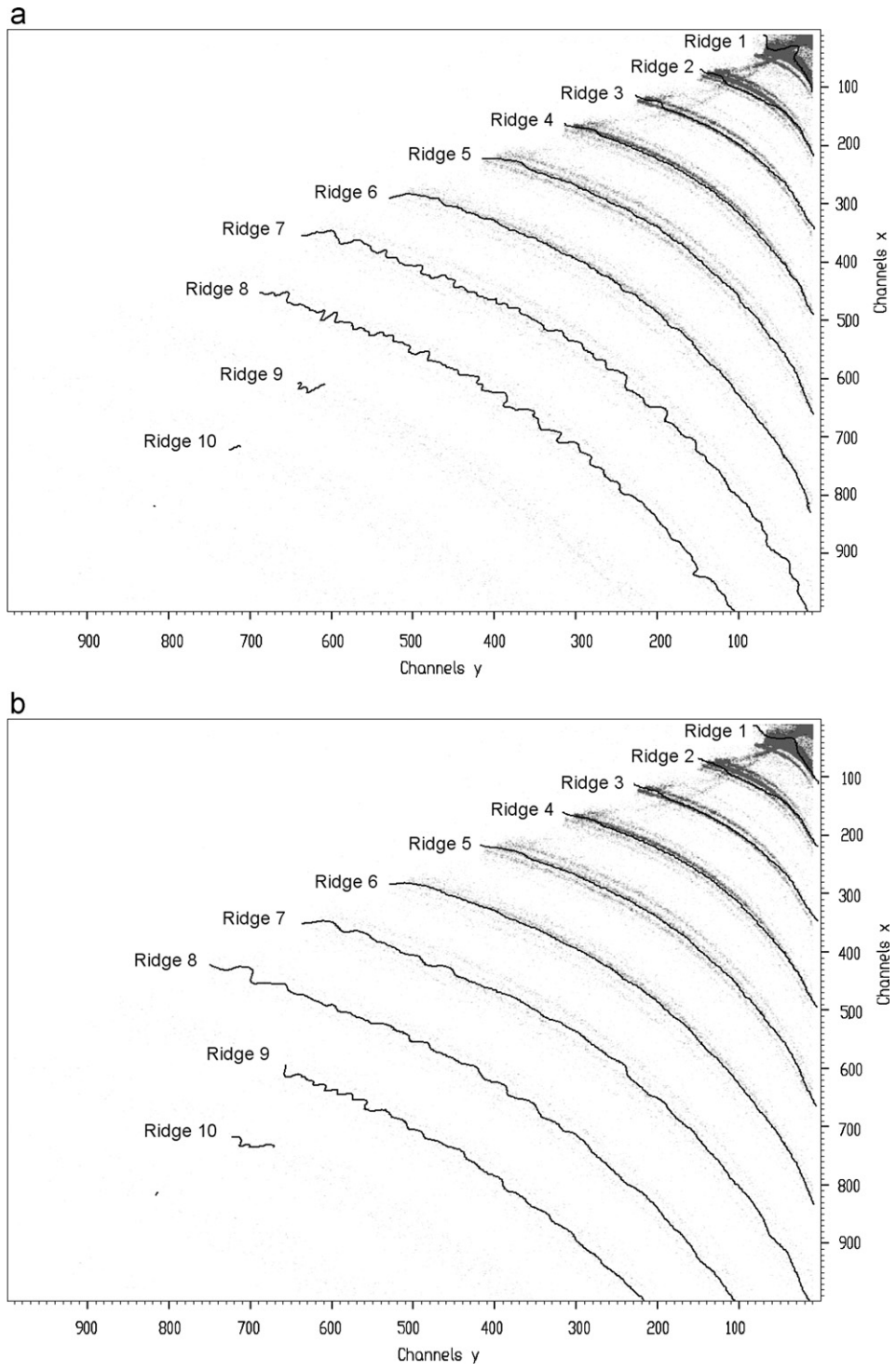

Fig. 15. Two-dimensional spectrum of nuclear multifragmentation with ridges estimated with parameters (a) $\sigma_3 = 5$, (b) $\sigma_3 = 10$, (c) $\sigma_3 = 20$ and (d) $\sigma_3 = 50$ ($\sigma_1 = 20$, $\sigma_2 = 30$, $\sigma_4 = 20$).

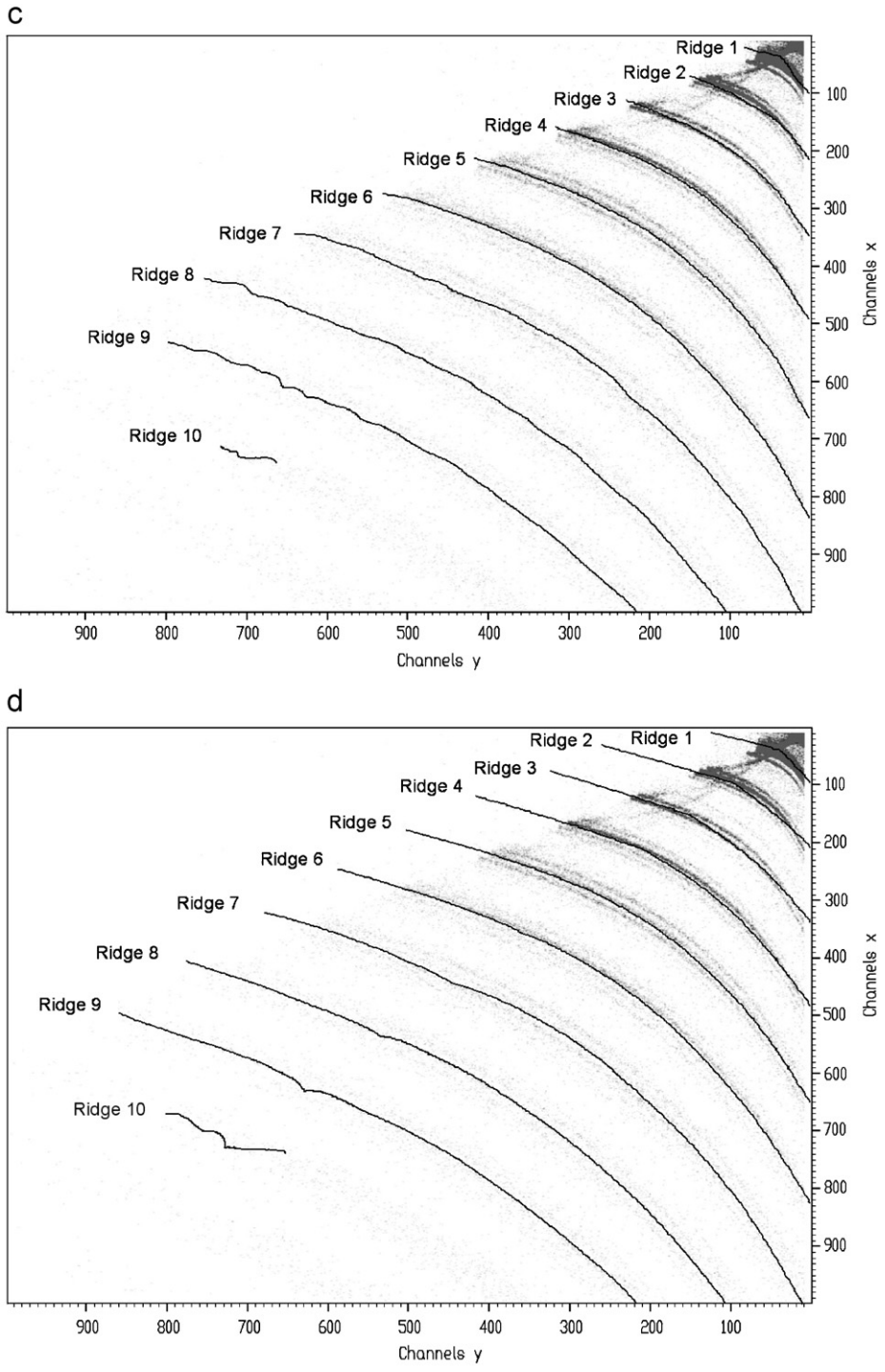

Fig. 15. (*Continued*)

ridges but it is unable to decompose and identify individual ridges of the clusters (see Fig. 1). By changing the parameter σ_4 in the last vertical filtration one can influence the width of identified ridges, or in other words to decompose them to subridges. In Fig. 16 we illustrate the results after application of the algorithm for $\sigma_4 = 10$ and 3. In Fig. 16a it discovers two subridges in the ridge 7 and identifies seeds of the ridges $R0$ and $R11$. When decreasing σ_4 to 3 we can decompose the main ridges to even more subridges. However, due to the loss of correlation among the points belonging to appropriate ridges, the lines are becoming shorter. The shape of lines fits better the original points in the spectrum than in Fig. 13.

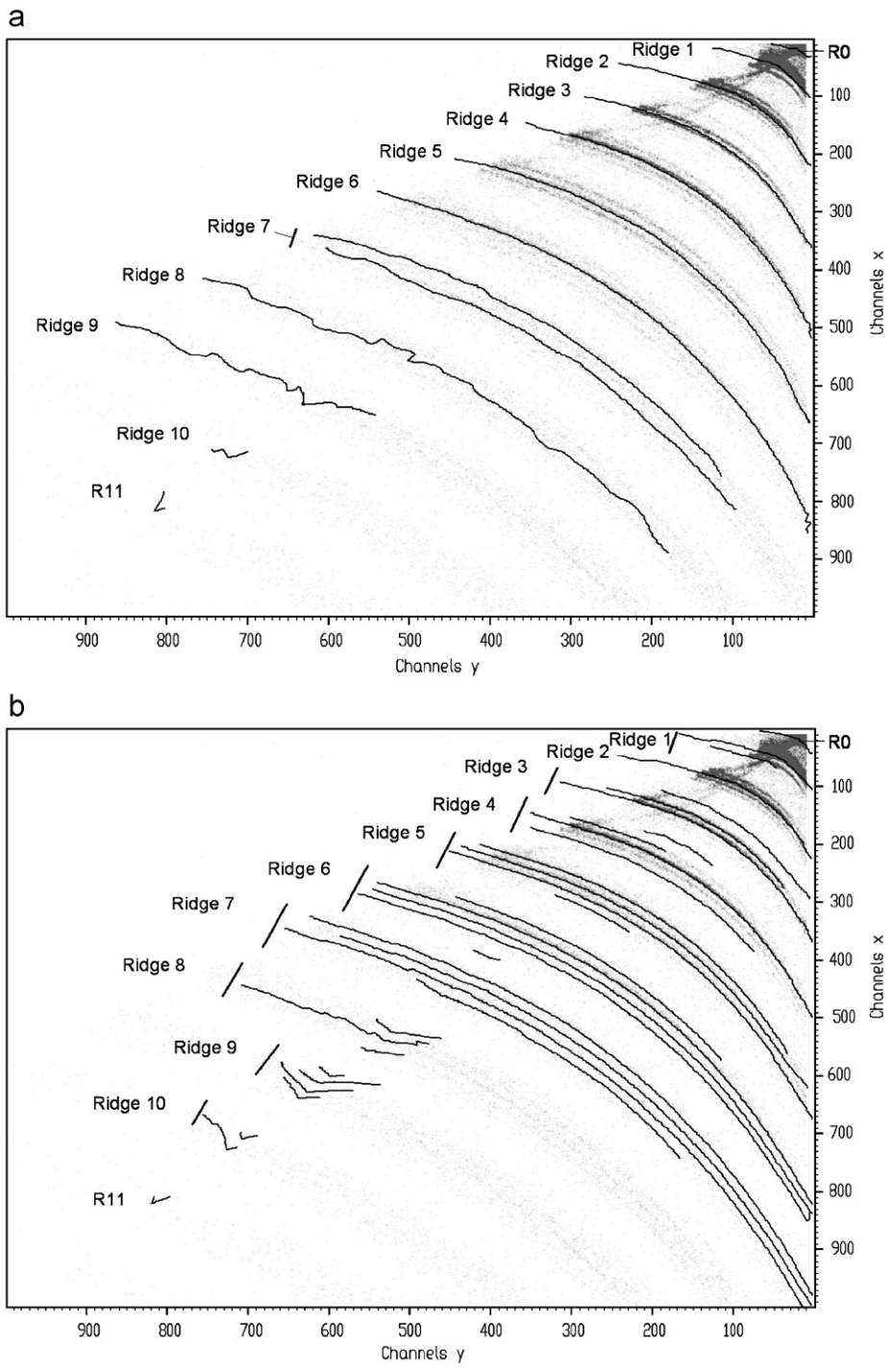

Fig. 16. Two-dimensional spectrum of nuclear multifragmentation with ridges estimated with parameters (a) $\sigma_4 = 10$ and (b) $\sigma_4 = 3$ ($\sigma_1 = 20$, $\sigma_2 = 30$, $\sigma_3 = 30$).

The other way to increase resolution in the estimation of ridges is to employ the operation of Gold deconvolution [13–15]. Analogously to the filtration in the columns of the data presented in Fig. 11 we slice the data in vertical direction. We get data similar to those presented in Fig. 8. Then for $\sigma = \sigma_d$ according to Eq. (2) we generate the second derivative of the Gaussian $c(j)$ and we take

$$r(j) = \begin{cases} -c(j) & \text{if } c(j) < 0 \\ 0 & \text{otherwise} \end{cases} \quad (6)$$

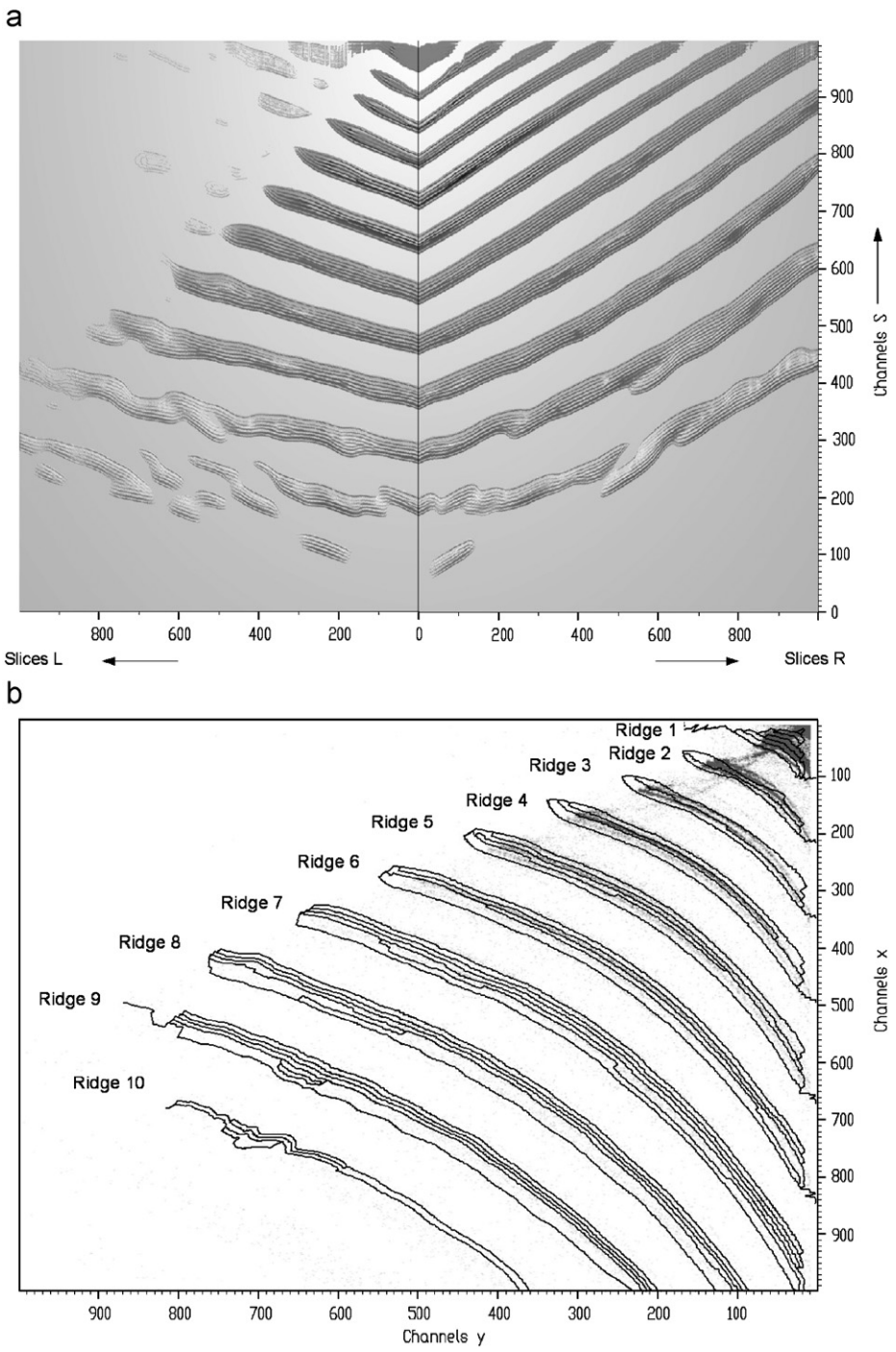

Fig. 17. (a) Data from Fig. 11 ($\sigma_1 = 20$, $\sigma_2 = 30$, $\sigma_3 = 30$, $\sigma_4 = 20$) after application of deconvolution operation to vertical slices ($\sigma_d = 5$) and (b) estimated decomposed slices transformed back to the two-dimensional spectrum of nuclear multifragmentation.

to be the response function (data similar to Fig. 5b). After application of the deconvolution algorithm for $\sigma_d = 5$ we obtain data shown in Fig. 17a. One can observe decomposition of main ridges to their components. After their identification and backward transformation to the space of original spectrum we present the result in Fig. 17b. Apparently the deconvolution operation decomposes the clusters of ridges.

The last free parameter in the estimation of ridges is threshold value, which influences the sensitivity of the algorithm. So far we have processed all the data with threshold value equal to 4%. Furthermore one can change

the starting point of the slicing according to Fig. 18. By now we have used the point A as the starting point of slicing.

In Fig. 19 we moved the starting point of slicing to the point A'. In the example we increased the length of the square to $l' = 2N$ and we changed the threshold value to 1%. One can observe that the identified ridges are smoother and the algorithm discovers also the ridge 11.

Until now we have analyzed 2D spectrum representing the telescope, consisting of two silicon detectors, given in Fig. 1. In Figs. 20 and 21 we present two other results of the identification of ridges in the telescope, consisting of one silicon detector followed by thick CsI scintillator crystal. Again good fidelity of the estimates of ridges can be observed.

Sometimes, e.g. for the 2D spectrum, obtained using CsI scintillator crystal via pulse shape discrimination technique, due to the course of the scattered data from the experiment it is necessary to change the starting point of the slicing. In the last example according to visual adjustment of the data we have moved it to the point C (see Fig. 18). Again good agreement of the estimated ridges with experimental measurements can be observed (Fig. 22).

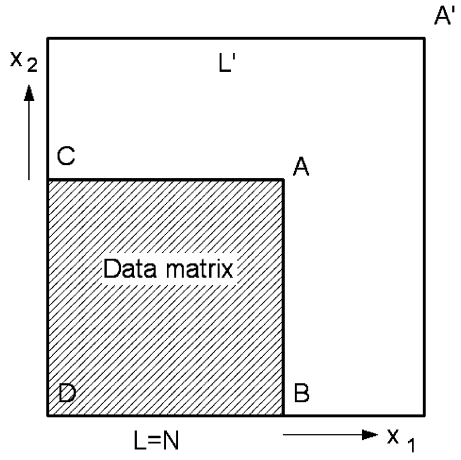

Fig. 18. Outline of choosing of starting point of slicing in two-dimensional spectrum.

4. Conclusion

An algorithm, allowing to automatically recognize isotope lines (manifested as non-linear ridges in the 2D spectra) in the 2D energy loss spectra of charged particles, is proposed in the present work.

The method presented in the work is a suitable extension of the method from [2], which after proper tuning can further minimize the human intervention, reducing it to supervision of the procedure. Due to its simplicity the method lends itself for the application during on-line acquisition where one often needs a preliminary fast evaluation of the yield.

The above described algorithm is rather simple and allows its realization on PC computers. Though the

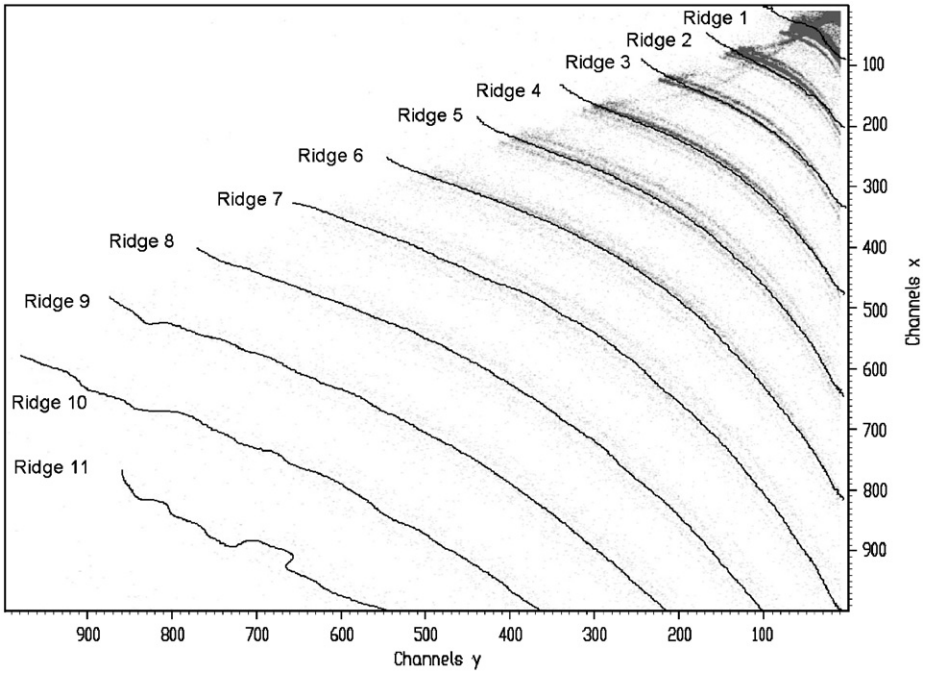

Fig. 19. Two-dimensional spectrum of nuclear multifragmentation with ridges estimated (threshold = 1%) with slicing started from at point A' ($\sigma_1 = 20$, $\sigma_2 = 30$, $\sigma_3 = 30$, $\sigma_4 = 20$).

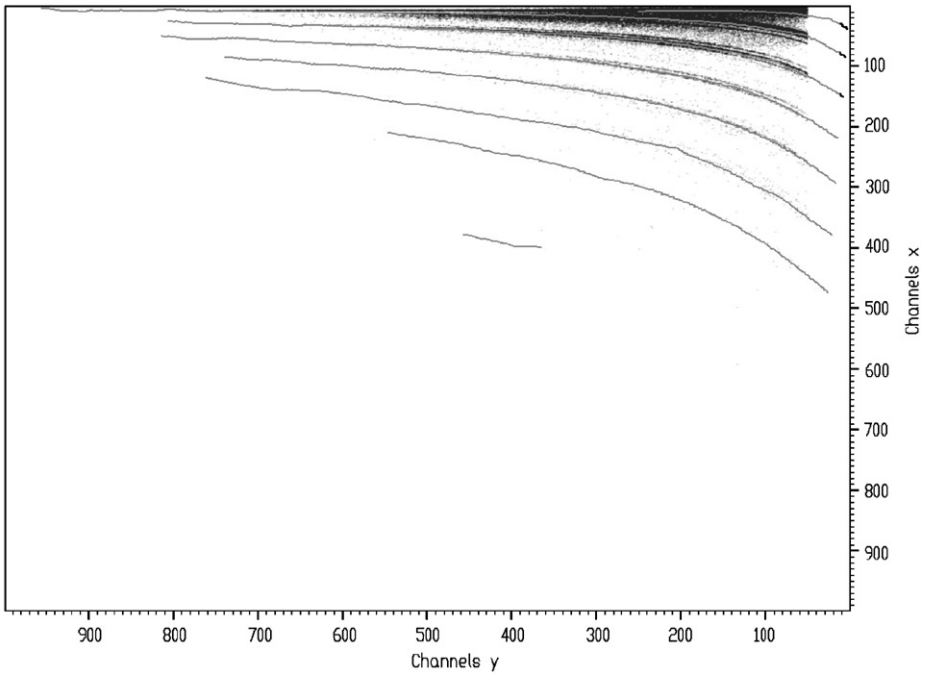

Fig. 20. Example of two-dimensional spectrum of nuclear multifragmentation with estimated ridges ($\sigma_1 = 20$, $\sigma_2 = 30$, $\sigma_3 = 30$, $\sigma_4 = 5$).

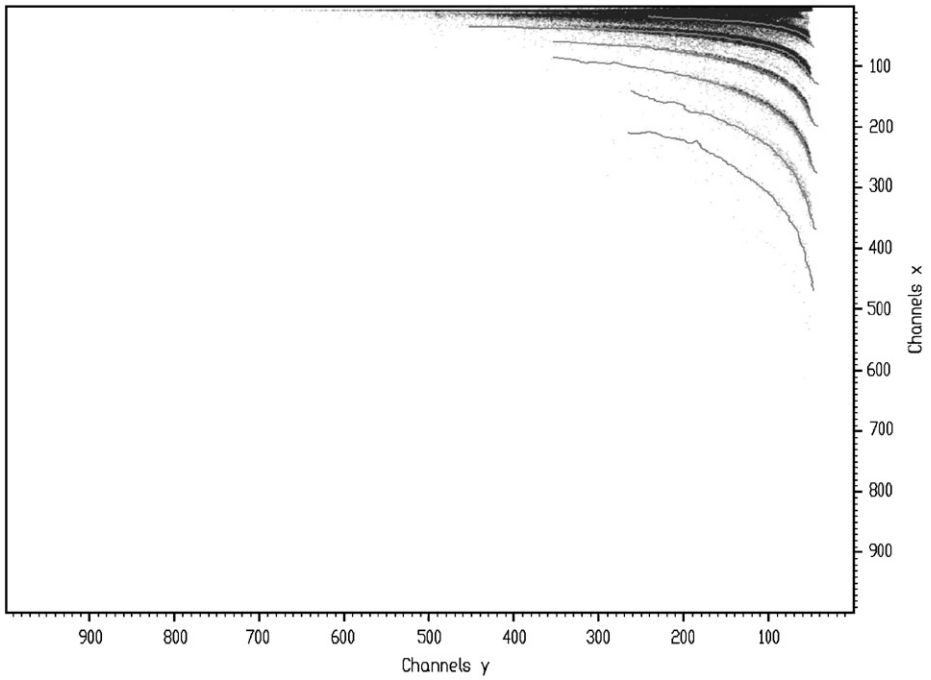

Fig. 21. Another example of two-dimensional spectrum of nuclear multifragmentation with estimated ridges ($\sigma_1 = 10$, $\sigma_2 = 10$, $\sigma_3 = 10$, $\sigma_4 = 5$).

procedure is fully automatic, due to large variability of the data, some intervention of the user and tuning of some parameters are required. The algorithm is rather fast. For example to process 2D spectrum with 1000×1000 channels it takes approximately 30 s (using PC, 3.2 GHz). However, when we include deconvolution procedure, which is time consuming operation, it takes, depending on number of iterations, several minutes (in our examples approximately 5 min). The method was implemented and integrated in DaqProVis system [16,17].

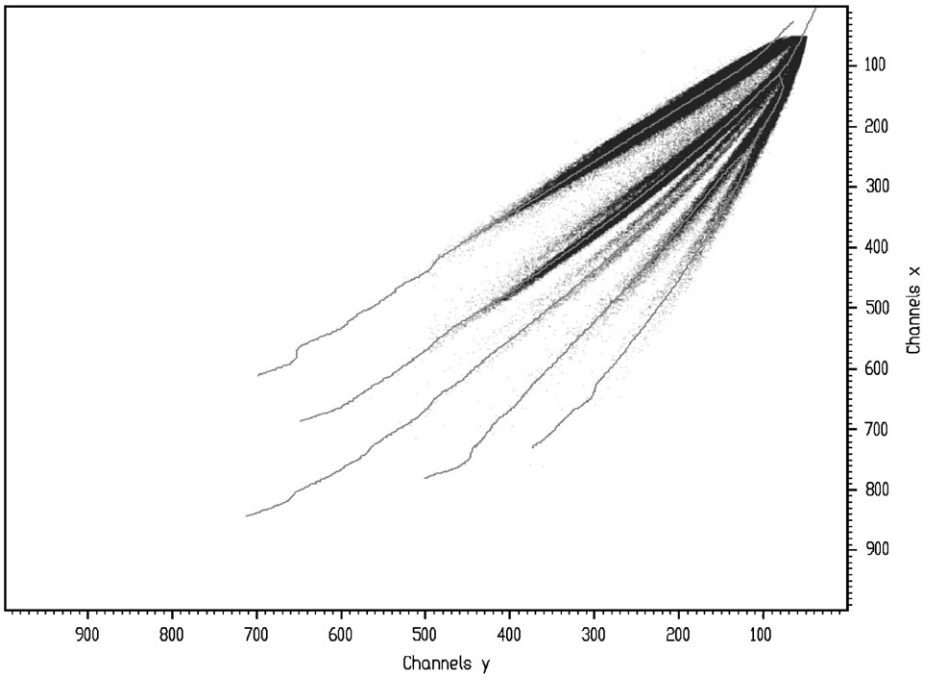

Fig. 22. Two-dimensional spectrum of nuclear multifragmentation with ridges estimated with slicing started at the point C ($\sigma_1 = 20$, $\sigma_2 = 30$, $\sigma_3 = 30$, $\sigma_4 = 10$).

Acknowledgements

This work was supported by Scientific Grant Agency through Project 2/7117/27 and 2/0073/08 from Ministry of Education of Slovak Republic and the Slovak Academy of Sciences.

References

[1] P.F. Mastinu, P.M. Milazzo, M. Bruno, M. D'Agostino, Nucl. Instr. and Meth. A 371 (1996) 510.
[2] M. Veselský, et al., Progress in Research, 2000–2001, Cyclotron Institute, Texas A&M University, College Station, 2001, p. V-32.; M. Veselský, Fiz. Elem. Chastits At. Yadra 36 (2005) 400; Phys. Part. Nuclei 36 (2005) 213.
[3] N. Leneindre, et al., Nucl. Instr. and Meth. A 490 (2002) 251.
[4] A. Benkirane, G. Auger, D. Bloyet, A. Chbihi, E. Plagnol, Nucl. Instr. and Meth. A 355 (1995) 559.
[5] M. Alderighi, et al., IEEE Trans. Nucl. Sci. NS-48 (2001) 385.
[6] C.V. Hampton, B. Lian, W.C. McHarris, Nucl. Instr. and Meth. A 353 (1994) 280.
[7] Z.K. Silagadze, Nucl. Instr. and Meth. A 376 (1996) 451.
[8] M.A. Mariscotti, Nucl. Instr. and Meth. A 50 (1967) 309.
[9] M. Morháč, J. Kliman, V. Matoušek, M. Veselský, I. Turzo, Nucl. Instr. and Meth. A 443 (2000) 108.
[10] M. Morháč, Nucl. Instr. and Meth. A 581 (2007) 821.
[11] W.W. Black, Nucl. Instr. and Meth. A 71 (1969) 317.
[12] J.T. Routti, S.G. Prussin, Nucl. Instr. and Meth. A 72 (1969) 125.
[13] R. Gold, ANL-6984, 1964.
[14] M. Morháč, J. Kliman, V. Matoušek, M. Veselský, I. Turzo, Nucl. Instr. and Meth. A 401 (1997) 385.
[15] M. Morháč, Nucl. Instr. and Meth. A 559 (2006) 119.
[16] M. Morháč, J. Kliman, V. Matoušek, I. Turzo, Nucl. Instr. and Meth. A 389 (1997) 89.
[17] M. Morháč, V. Matoušek, I. Turzo, J. Kliman, Nucl. Instr. and Meth. A 559 (2006) 76.